Sensitivity Analysis of Disturbance Accommodating Control with Kalman Filter Estimation

Jemin George* and John L. Crassidis†

University at Buffalo, State University of New York, Amherst, NY, 14260-4400

The design of controllers that can automatically compensate the effects of uncertain disturbances in a system has become an important topic in modern control engineering. The general theory of disturbance accommodating control provides a method for designing feedback controllers which automatically detect and minimizes the effect of waveform-structured disturbances. This approach has been applied on linear systems with small modeling errors and uncertainties. Based on the disturbance accommodating control theory, a control technique for nonlinear systems with time-varying modeling errors and uncertainties is presented in this paper. This control approach exploits an Extended Kalman Filter for the simultaneous estimation of the system states and the uncertain disturbances. Validity of this control approach is verified by implementing the proposed technique on a highly nonlinear wing-rock system. The simulation results indicated that the closed-loop stability of the controlled system is extremely sensitive to the user selected process noise covariance value. A Lyapunov stability analysis is conducted on a controlled linear system, which reveals a lower bound requirement on the process noise covariance norm to facilitate the asymptotic stability of the closed-loop system. This lower bound on the process noise covariance norm depends on the model uncertainties, external disturbances and the amount of noise associated with the measurements.

I. Introduction

EVERY real system has uncertainties, which include system parametric uncertainties, unmodeled dynamics and external disturbances. Also, the available information from measurements, i.e. sensor outputs, usually does not contain full state information and is most often corrupted by noise. The presence of uncertainty and noise could obscure the development of a control law. Several robust control strategies have been developed to keep the performance within acceptable ranges in the presence of uncertainty, e.g. H_∞ Control, μ-Synthesis, Adaptive Control, etc. Each method has its own advantages and disadvantages.

In 1971 Johnson introduced a new technique for accommodating disturbance in a linear quadratic regulator problem.[1] This new technique, known as the Disturbance Accommodating Control (DAC), is concerned with the design of feedback controllers which can maintain set-point regulation or servo-tracking in the face of uncertain external disturbance. There are three modes in which the disturbance accommodating controller can operate; disturbance absorption mode, disturbance minimization mode, and disturbance utilization mode.[2] The general formulation of DAC only considers disturbance functions which exhibit waveform patterns over short intervals of time in contrast to noise type disturbances. Mathematical models of waveform structured disturbance can be easily developed since these types of disturbances are assumed to be the output of a physical system whose inputs are sparsely populated sequences of impulses.

Adaptive controller design using disturbance accommodation techniques is first presented in Ref. 3. These adaptive controllers can automatically compensate for uncertain plant-parameter perturbations as well as external disturbance inputs. Design of an adaptive disturbance accommodating controller which utilizes a full order Luenberger observer for disturbance estimation is presented in Ref. 4. This adaptive control technique has been successfully applied to nonlinear systems by first linearizing the plant about a set point and then computing the control law for the corresponding linear system. Adaptive controller for the rejection of persistent disturbances for continuous and discrete systems is presented in Ref. 5. This control approach

*Graduate Student, Department of Mechanical & Aerospace Engineering, jgeorge3@buffalo.edu, Student Member AIAA.
†Professor, Department of Mechanical & Aerospace Engineering, johnc@buffalo.edu, Associate Fellow AIAA.

is based on developing adaptive laws for feedback gains that will ensure the asymptotic stability of the closed-loop system. These adaptive controller formulations assume noise-free full state feedback, which is highly unrealistic.

A technique for disturbance estimation and compensation which produces a control scheme that has zero steady-state tracking error to finite-dimensional deterministic disturbance is presented in Ref. 6. The structure of the discrete-time disturbance estimator shown in Ref. 6 requires two separate suboptimal estimators. Implementation of a discrete-time Kalman filter to estimate disturbance using sliding mode is presented in Ref. 7. Both of these disturbance estimation techniques are limited to linear systems.

A nonlinear robust control approach known as the Model Error Control Synthesis (MECS), which mitigates the effects of model errors and external disturbance on a system by providing corrections to the nominal control input is presented in Ref. 8. The MECS technique uses an estimator based on the predictive filter approach for determining modeling errors and external disturbance inputs. The main advantage of MECS approach over DAC is that the MECS approach does not assume any specific structure for the disturbance process and the true state vector does not needed to be appended in MECS to estimate for the disturbance. Recent research has shown that the existence of noise in the feedback loop can results in poor disturbance predictions by the predictive filter and thus result in degradation of closed-loop system performance.

This paper presents a robust control approach for nonlinear systems based on the DAC theory. This control scheme exploits an Extended Kalman Filter (EKF) for simultaneously estimating the system states and the disturbance term from the noisy measurement signal. A control law is then developed based on the estimated states and disturbance. The accuracy of Kalman filter estimates are directly related to the process noise covariance and the measurement noise covariance values. The measurement noise covariance can easily be determined based on the sensors while the process noise covariance behaves like a tuning parameter. The main objective of this paper is to investigate the sensitivity of the closed-loop stability of a controlled system to the process noise covariance.

The paper is organized as follows. First, the formulation of an EKF for the simultaneous estimation of system states and disturbance is presented, followed by the implementation of the DAC method using the EKF approach on a highly nonlinear wing rock system. A Lyapunov stability analysis is then conducted on a linear system which utilizes a linear continuous-time Kalman filter for disturbance estimation. Lyapunov stability analysis is concluded with the formulation of a lower bound requirement on the process noise covariance norm in order for the controlled system to be asymptotically stable. A stability analysis is then conducted on a linearized wing rock system which utilizes a linear continuous-time Kalman filter for disturbance estimation. Finally, numerical simulation results which authenticate the Lyapunov stability analysis are provided.

II. Disturbance Accommodating Controller for Nonlinear Systems: An Extended Kalman Filter Approach

Most nonlinear control strategies require full state knowledge, but the available information from measurements, i.e., sensor outputs, usually does not contain full state information and is often corrupted by noise. Also, the uncertainties in system nonlinearities and the presence of external disturbance can further complicate the implementation of a control scheme. Design methodology of a disturbance accommodating controller which utilize an EKF for the simultaneous estimation of the system states and disturbance from noisy measurement signal is presented in this section. This formulation is based on the idea that all the system uncertainties can be lumped into an external disturbance term. Estimated disturbance can then be used to make necessary corrections to the nominal control input to achieve robust performance in the presence of uncertainties and disturbance.

Consider a discrete time nonlinear stochastic difference equation

$$\mathbf{x}_k = \mathbf{f}(\mathbf{x}_{k-1}, \mathbf{u}_{k-1}, \mathbf{w}_{k-1}) \tag{1}$$

with a measurement $\mathbf{y}_k \in \Re^m$, i.e.,

$$\mathbf{y}_k = \mathbf{h}(\mathbf{x}_k, \mathbf{v}_k) \tag{2}$$

where variables $\mathbf{w}_k$ and $\mathbf{v}_k$ represent the disturbance and measurement noise, respectively. They are assumed

to be independent of each other, zero-mean, white and with normal probability distribution, i.e.

$$\begin{aligned} p(\mathbf{w}_k) &\sim N(0, Q_k), \\ p(\mathbf{v}_k) &\sim N(0, R_k) \end{aligned} \tag{3}$$

Based on the DAC theory,[9] the disturbance process can be modeled as

$$\begin{aligned} \mathbf{w}_{k-1} &= \boldsymbol{\mathcal{W}}(\mathbf{x}_{k-1}, \mathbf{z}_{k-1}) \\ \mathbf{z}_k &= \boldsymbol{\mathcal{Z}}(\mathbf{x}_{k-1}, \mathbf{z}_{k-1}) + \boldsymbol{\sigma}_{k-1} \end{aligned} \tag{4}$$

where $\mathbf{z}_k$ represents the state vector of the disturbance process and $\boldsymbol{\sigma}_k$ represents a sequence of random intensity and sparsely-spaced impulse functions, in other words the noise associated with disturbance process. Now the following extended state vector $\mathbf{X}_k$ is introduced:

$$\mathbf{X}_k = \begin{bmatrix} \mathbf{x}_k \\ \mathbf{z}_k \end{bmatrix} \tag{5}$$

Combining Eqs. (1) and (4), the aggregated stochastic difference equation can be expressed as

$$\mathbf{X}_k = \begin{bmatrix} \mathbf{f}(\mathbf{x}_{k-1}, \mathbf{u}_{k-1}, \mathbf{w}_{k-1}) \\ \boldsymbol{\mathcal{Z}}(\mathbf{x}_{k-1}, \mathbf{z}_{k-1}) + \boldsymbol{\sigma}_{k-1} \end{bmatrix} = \boldsymbol{\mathcal{F}}(\mathbf{X}_{k-1}, \mathbf{u}_{k-1}, \boldsymbol{\sigma}_{k-1}) \tag{6}$$

and the measurement equation can be expressed as

$$\mathbf{Y}_k = \boldsymbol{\mathcal{H}}(\mathbf{X}_k, \mathbf{v}_k) \tag{7}$$

In the EKF approach, after declaring an initial state estimate, $\hat{\mathbf{X}}_0^-$, and error covariance matrix, P_0^-, the Kalman gain can be calculated as

$$K_k = P_k^- H_k^T \Big(H_k P_k^- H_k^T + R_k \Big)^{-1} \tag{8}$$

where H_k is the Jacobian matrix of partial derivatives of $\boldsymbol{\mathcal{H}}$ with respect to $\mathbf{X}_k$ and R_k is the discrete-time measurement noise covariance matrix. The superscripts $-$ and $+$ represent the predicted and updated values, respectively. Having calculated the Kalman gain, the predicted state vector and covariance matrix are updated using the equations

$$\hat{\mathbf{X}}_k^+ = \hat{\mathbf{X}}_k^- + K_k(\mathbf{Y}_k - H_k \hat{\mathbf{X}}_k^-) \tag{9}$$

$$P_k^+ = (I - K_k H_k) P_k^- \tag{10}$$

After updating the predictions, the estimates are propagated to the next time-step using

$$\hat{\mathbf{X}}_{k+1}^- = \boldsymbol{\mathcal{F}}(\hat{\mathbf{X}}_k^+, \mathbf{u}_k, \mathbf{0}) \tag{11}$$

$$P_{k+1}^- = A_k P_{k-1}^+ A_k^T + W_k Q_k W_k^T \tag{12}$$

where A_k is the Jacobian matrix of partial derivatives of $\boldsymbol{\mathcal{F}}$ with respect to $\mathbf{X}_k$ and W_k represents the Jacobian matrix of partial derivatives of $\boldsymbol{\mathcal{F}}$ with respect to $\boldsymbol{\sigma}_k$.

Note that the updated extended state vector in Eq. (9) contains a numerical approximation to the disturbance. This information can be used to correct the control input into the system using the relation[8]

$$\mathbf{u}_k = \bar{\mathbf{u}}_k - \hat{\mathbf{z}}_{k-1}^+ \tag{13}$$

where $\bar{\mathbf{u}}$ represents the nominal control input and $\hat{\mathbf{z}}^+$ represents the updated states of the disturbance process. There is a time delay present in this formulation because the measurement vector, $\mathbf{Y}_k$, must be given before the disturbance in the system can be updated using Eq. (9).

III. Wing Rock Suppression of Slender Delta Wing

In this section, the implementation of the DAC approach using a discrete-time EKF to suppress the wing rock motion of a slender delta wing is presented. More detailed formulation of this problem can be found in Ref. 8. Wing rock represents a self-induced limit cycle oscillation in the presence of some initial disturbance or asymmetry in the flow field. The primary causes of wing rock are the interactions between the forebody and the wing vortices at high angle of attack.[10] This has been verified using video-based experimental investigation for wing rock of sharp-edged delta wings with leading-edge sweep angles of 70° and 80°.[11] In order to predict roll divergence as well as other characteristics in the oscillation, a highly nonlinear analytical models of wing rock has been developed.[12]

Wing rock can be controlled using numerous control schemes such as optimal control methods,[13] adaptive control using backstepping[14] and variable structure adaptive control.[15] One of the difficult aspects in the control of wing rock motion is the extreme sensitivity to parameter variations. A slight change in system parameter can drastically affect overall system performance. Disturbance inputs, which can adversely affect closed system performance, were not considered in above control schemes. However, satisfactory wing rock motion control can be achieved by the DAC approach presented here.

The wing rock equation of motion for slender delta wings is given by:[12]

$$\dot{\phi}(t) = p(t) \tag{14}$$

$$\dot{p}(t) = c_1 + c_2\phi(t) + c_3 p(t) + c_4|\phi(t)|p(t) + c_5|p(t)|p(t) + c_6 u(t) + w(t) \tag{15}$$

The measurement equation is:

$$y(t) = \mathbf{h}(\mathbf{x}(t), t) + v(t) \tag{16}$$

$$= \phi(t) + v(t) \tag{17}$$

The wing-rock system consist of two states, roll-angle (ϕ) and roll-angle rate (p). According to Eq. (17), roll-angle is the only measurable state and roll-angle rate needs to be estimated from the noisy roll-angle measurements. The control objective is to suppress an initial roll-angle of 30° within 2 seconds. A variable structure controller (VSC) can be designed to achieve this requirement for a no disturbance, no noise, and full state knowledge scenario. For VSC, the control law can be calculated as

$$\begin{aligned}\bar{u}(t) = -\frac{1}{\bar{c}_6}\Big(\bar{c}_1 + \bar{c}_2\phi(t) + \bar{c}_3 p(t) + \bar{c}_4|\phi(t)|p(t) + \bar{c}_5|p(t)|p(t)\Big) \\ + \frac{1}{\bar{c}_6}\Big\{ - \vartheta p(t) - \eta \mathrm{sat}\Big[\frac{p(t) + \vartheta\phi(t)}{\rho}\Big]\Big\}\end{aligned} \tag{18}$$

where $\bar{c}_i$ represents the assumed system parameters. The assumed values of system parameters, $\bar{c}_i$, for $i = 1, 2, \ldots, 6$ are chosen for an angle of attack of 30° as follows:[8]

$$\bar{c}_1 = 5, \bar{c}_2 = -26.7, \bar{c}_3 = 0.765, \bar{c}_4 = -2.9, \bar{c}_5 = -2.5, \bar{c}_6 = 0.75 \tag{19}$$

In Eq. (18), ϑ, η, and ρ are design parameters and to meet the design goal, the following values are used:[8]

$$\vartheta = 10, \eta = 3, \rho = 0.1 \tag{20}$$

The saturation function, $\mathrm{sat}(\cdot)$, is defined by

$$\mathrm{sat}(x) \equiv \begin{cases} x & \text{if } |x| \le 1 \\ \mathrm{sgn}(x) & \text{otherwise} \end{cases} \tag{21}$$

where the signum function, $\mathrm{sgn}(\cdot)$, is defined by

$$\mathrm{sgn}(x) \equiv \begin{cases} 1 & \text{for } x > 0 \\ 0 & \text{for } x = 0 \\ -1 & \text{for } x < 0 \end{cases} \tag{22}$$

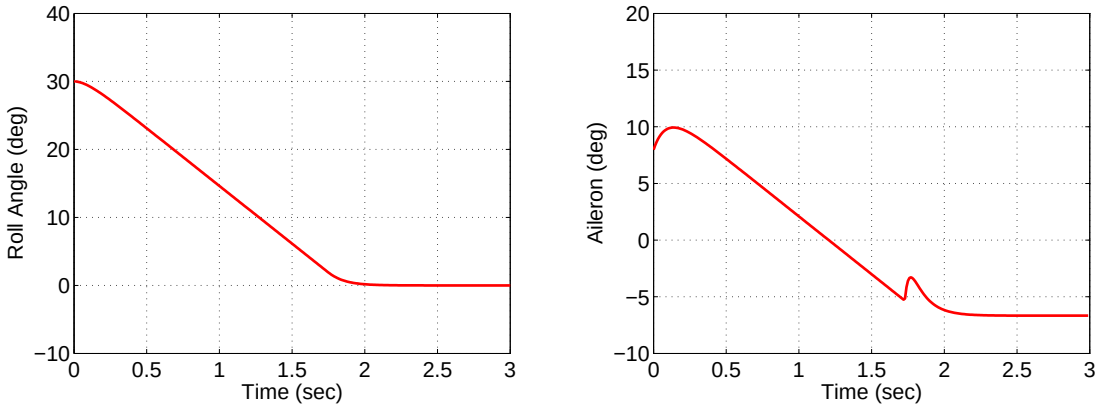

(a) System Response (Roll Angle)

(b) Control Input (Aileron Deflection)

Figure 1. System Response and Control Input for Variable Structure Controller

A plot of the system response and the control input obtained using the variable structure controller with no disturbance and noise are given in Fig. 1. Clearly, the variable structure controller meets the desired specifications when there is no noise and disturbance.

Now consider a case where "disturbance"and noise are present. Let's assume that the uncertainties in system parameters constitute for the disturbance. The noise is assumed to be zero-mean white noise with a standard deviation of 0.0013^{o}, i.e., the discrete-time measurement error covariance $R_k = 5 \times 10^{-12}$. Now an EKF can be implemented to estimate the system states and the disturbance. First, the following extended state vector is formed:

$$\mathbf{X}(t) = \begin{bmatrix} \phi(t) \\ p(t) \\ z(t) \end{bmatrix} \tag{23}$$

The aggregated continuous-time state equation can be expressed as

$$\dot{\mathbf{X}}(t) = \begin{bmatrix} p(t) \\ \bar{c}_1 + \bar{c}_2\phi(t) + \bar{c}_3 p(t) + \bar{c}_4|\phi(t)|p(t) + \bar{c}_5|p(t)|p(t) + \bar{c}_6\bar{u}(t) - \bar{c}_6 z(t) \\ \sigma(t) \end{bmatrix} \tag{24}$$

where $\bar{u}(t)$ represents the nominal control input from Eq. (18) and $\sigma(t)$ as mentioned earlier, represents the noise associated with the disturbance process. Notice that Eq. (24) assumes that there is no dynamics associated with the disturbance process. After substituting Eq. (18) into Eq. (24), the Jacobian matrix of partial derivatives of the aggregated state equation with respect to $\mathbf{X}(t)$ can be calculated as

$$F = \begin{bmatrix} 0 & 1 & 0 \\ -300 & -40 & -\bar{c}_6 \\ 0 & 0 & 0 \end{bmatrix}$$

and the Jacobian matrix of partial derivatives of the aggregated state equation with respect to $\sigma(t)$ can be calculated as

$$G = \begin{bmatrix} 0 & 0 & 1 \end{bmatrix}^T$$

Now the following 6×6 matrix, $\mathbb{A}$ is formed:

$$\mathbb{A} = \begin{bmatrix} -F & GQG^T \\ 0 & F^T \end{bmatrix} \Delta t \tag{25}$$

where $\triangle t$ is the constant sampling interval and Q is the constant continuous-time process noise covariance. The matrix exponential of $\mathbb{A}$ can be calculated as

$$\mathcal{B} = e^{\mathbb{A}} = \begin{bmatrix} \mathcal{B}_{11} & \mathcal{B}_{12} \\ 0 & \mathcal{B}_{22} \end{bmatrix} \quad = \begin{bmatrix} \mathcal{B}_{11} & A_k^{-1}\mathcal{Q}_k \\ 0 & A_k^T \end{bmatrix} \tag{26}$$

where A_k is the state transition matrix of F and $\mathcal{Q}_k$ represents the quantity $W_k Q_k W_k^T$ from Eq. (12). According to Eq. (17), roll-angle is the only measurable state and therefore the Jacobian matrix H_k can be computed as

$$H_k = \begin{bmatrix} 1 & 0 & 0 \end{bmatrix}$$

The control objective is to suppress an initial roll-angle of 30° and therefore the initial extended state estimates are given as

$$\hat{\mathbf{X}}_0^- = \begin{bmatrix} \frac{\pi}{6} & 0 & 0 \end{bmatrix}^T$$

and the initial error covariance is selected as

$$P_0^- = \begin{bmatrix} \left(\frac{\pi}{18}\right)^2 & 0 & 0 \\ 0 & \left(\frac{0.01}{3}\right)^2 & 0 \\ 0 & 0 & 50 \end{bmatrix}$$

The relatively large third diagonal element represents the large uncertainty in initial disturbance prediction. Knowing the initial error covariance matrix, the Kalman gain can be computed using Eq. (8). Now the initial extended state estimates and the initial error covariance matrix can be updated using Eqs. (9) and (10), respectively. Using the updated state estimates the nominal control input can be calculated using Eq. (18) and necessary corrections to the nominal control input can be made using Eq. (13). Using the assumed system dynamics, the extended states can be propagated forward in time while the error covariance can be propagated using the equation

$$P_{k+1}^- = A_k P_{k-1}^+ A_k^T + \mathcal{Q}_k \tag{27}$$

A block diagram of the controlled system with EKF for state and disturbance estimation is given in Fig. 2. Notice that the variable structure controller uses the updated states to calculate the nominal control input.

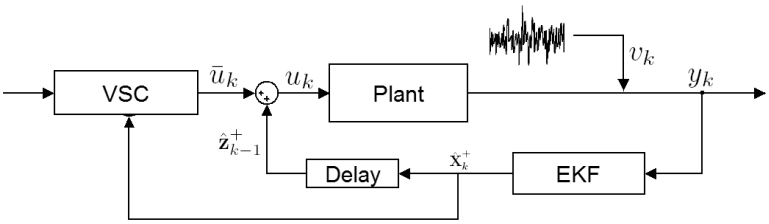

Figure 2. Disturbance Accommodating Controller with Extended Kalman Filter

IV. Simulation Results

Simulation results obtained by implementing the DAC scheme with discrete-time EKF in wing rock suppression example are given in this section. Simulations are conducted for five different scenarios given below:

1. No uncertainty/disturbance scenario
2. Disturbance from uncertainties in time-varying system parameters, i.e. $c_1 = 5\sin(15t)$, $c_2 = -26.7$, $c_3 = 0.765$, $c_4 = 3\cos(5t)$, $c_5 = 10\sin(10t)$, and $c_6 = 0.75$
3. Disturbance from an increase in input value (c_6), i.e. $c_6 = \frac{4}{3} \times \bar{c}_6$

4. Disturbance from a decrease in input value (c_6), i.e. $c_6 = \frac{2}{3} \times \bar{c}_6$

5. Disturbance from both uncertainties in time-varying system parameters and an increase in input value (c_6), i.e. a combination of case 2 and 3.

In order to compare the system roll-angle response obtained, it is compared against the desired response shown in Fig. 1(a). Also, the norm of the difference between the desired and actual system roll-angle response is calculated to quantify the controller validation. Comparing the error norm along with the system response plots and the control input plots will provide an accurate evaluation of the DAC approach using discrete-time EKF.

The process noise covariance, Q, is a tuning parameter and tuning Q to the optimal value will result in the best possible disturbance predictions. First, for each disturbance scenario discussed earlier, multiple simulations are conducted using different process noise covariance values. The optimal process noise covariance value is selected to be the one that results in the lowest respective error norm. Given in Table 1 are the different process noise covariance values and the corresponding error norm for all five scenarios. The results shown in Table 1 indicate that the error norm reaches a steady value as the process noise covariance value increases beyond 1.0×10^{15}. Also, as the covariance value decreases beyond 1.0, the error norm increases. Based on data shown, one could see that for most disturbance scenarios, except for case one, the minimum error norm is obtained when the covariance value is selected to be 1.0×10^{15}. The maximum error norm is obtained when the covariance is less than 1.0×10^{-15}. For each disturbance scenario, simulations are first conducted using two different covariance values that correspond to the maximum and the minimum error norms.

Table 1. Process Noise Covariance vs. Error Norm

Q	Case 1	Case 2	Case 3	Case 4	Case 5
1.0×10^{-50}	26.5050	320.4538	183.7198	41.7888	422.9094
1.0×10^{-25}	26.5050	320.4538	183.7198	41.7888	422.9094
1.0×10^{-20}	26.5050	320.4538	183.7198	41.7888	422.9094
1.0×10^{-15}	26.5050	320.4538	183.7198	41.7888	422.9094
1.0×10^{-10}	26.5064	320.4658	183.7199	41.7923	422.9089
1.0×10^{-08}	26.6393	321.6458	183.7184	42.1483	422.8575
1.0×10^{-06}	53.2364	355.1636	208.1468	88.7171	414.1562
1.0×10^{-05}	115.3542	357.3103	278.1453	152.7620	423.0938
1.0×10^{-04}	136.2656	273.8644	257.8684	103.5785	338.7352
1.0×10^{-03}	84.8338	163.1424	188.8328	25.1979	225.2172
1.0×10^{-02}	15.3385	53.2804	112.0110	3.6850	128.4052
1.0×10^{-01}	0.0818	6.8449	27.6116	2.7049	44.4345
$1.0 \times 10^{+00}$	0.0371	5.9245	1.2822	2.2401	4.3847
$1.0 \times 10^{+01}$	0.0459	5.3450	1.1603	1.8852	3.8556
$1.0 \times 10^{+02}$	0.0676	4.2923	0.9572	1.5142	2.9880
$1.0 \times 10^{+03}$	0.2541	2.9710	0.7420	1.2139	2.0179
$1.0 \times 10^{+04}$	0.2652	2.2734	0.6021	1.1684	1.3735
$1.0 \times 10^{+05}$	0.2282	2.2227	0.5845	1.1601	1.3261
$1.0 \times 10^{+07}$	0.2233	2.2196	0.5825	1.1591	1.3251
$1.0 \times 10^{+10}$	0.2233	2.2195	0.5825	1.1591	1.3251
$1.0 \times 10^{+15}$	0.2245	2.2150	0.5817	1.1580	1.3219
$1.0 \times 10^{+20}$	0.2840	2.8222	0.7413	1.4823	1.7648
$1.0 \times 10^{+25}$	0.2840	2.8222	0.7413	1.4823	1.7648
$1.0 \times 10^{+50}$	0.2840	2.8222	0.7413	1.4823	1.7648
$1.0 \times 10^{+100}$	0.2840	2.8222	0.7413	1.4823	1.7648

A. Simulation Results for Case 1

Given in Fig. 3 are the system responses obtained by implementing the DAC approach with discrete-time EKF on the wing rock example using two different process noise covariance values. The results shown in Fig. 3 indicate that the closed-loop system is unstable if the process noise covariance is selected to be 1.00×10^{-15}. The overall system performance is very similar to the desired performance if the process noise covariance is selected to be 1.00×10^{15}.

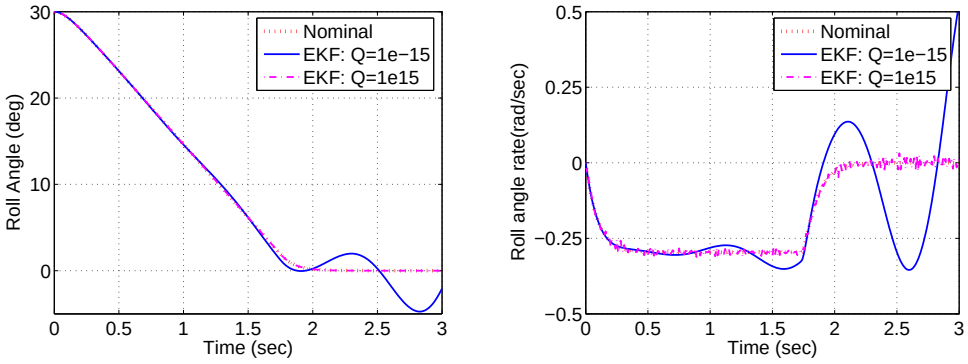

(a) System Response(Roll Angle) (b) System Response(Roll Angle rate)

Figure 3. System Response for Case 1.

The estimated disturbances for both process noise covariance values are given in Fig. 4(a). Since case one investigates the no uncertainty/disturbance scenario, the true disturbance is close to zero, but the estimated disturbance is highly noisy if the process noise covariance is selected to be 1.00×10^{15}. The control inputs or the aileron deflections are shown in Fig. 4(b). The control input for process noise covariance, $Q = 1.00 \times 10^{15}$, is highly noisy. On the other hand, the control input for process noise covariance, $Q = 1.00 \times 10^{-15}$, is noise free but it is much different from the nominal control input.

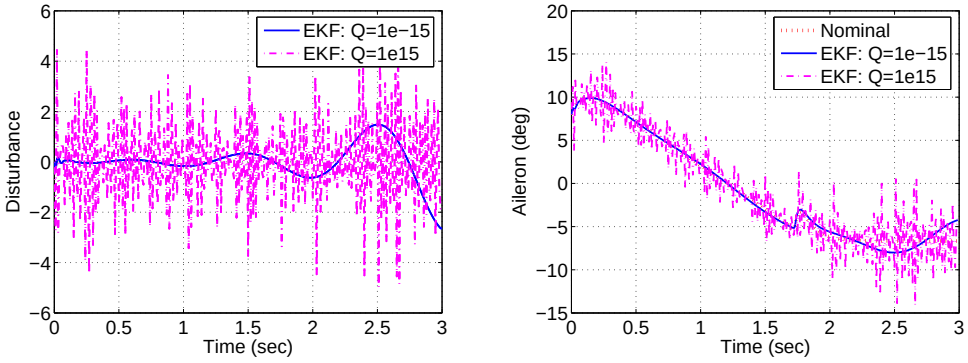

(a) Disturbance (b) Control Input

Figure 4. Disturbance and Control Input for Case 1.

B. Simulation Results for Case 2

Figure 5 compares the system responses obtained from the DAC approach with discrete-time EKF to the desired response for the case two disturbance scenario. Figures 5(a) and 5(b) indicates that the the closed-loop system is unstable if the process noise covariance is selected to be 1.00×10^{-15}.

The estimated disturbances for both process noise covariance values are given in Fig. 6(a). Since case two involves time varying system parameters, the estimated disturbance is also time varying. The estimated disturbance is highly noisy if the process noise covariance is selected to be 1.00×10^{15}. The control inputs

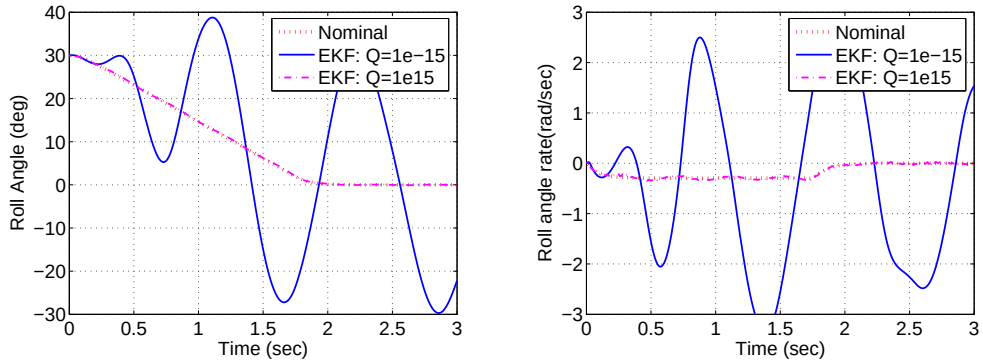

(a) System Response(Roll Angle) (b) System Response(Roll Angle rate)

Figure 5. System Response for Case 2.

or the aileron deflections for both process noise covariance values are shown in Fig. 6(b). The control input for process noise covariance, $Q = 1.00 \times 10^{15}$, is also highly noisy.

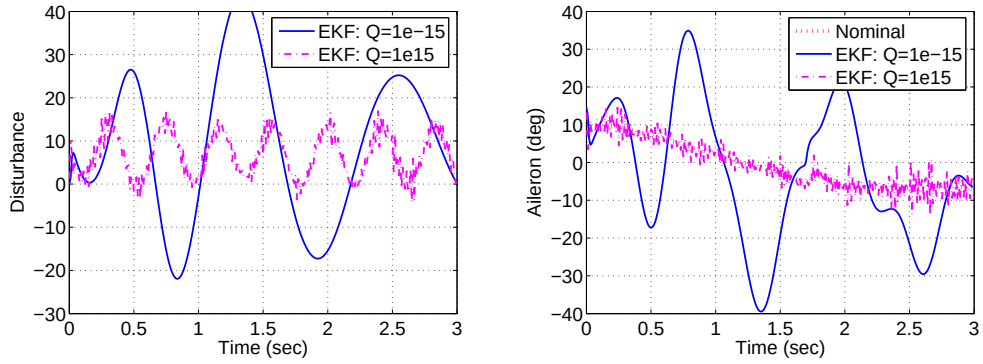

(a) Disturbance (b) Control Input

Figure 6. Disturbance and Control Input for Case 2.

C. Simulation Results for Case 3

In case 3, the DAC approach with a discrete-time EKF is implemented on a system where the disturbance is induced by an increase in the input value (c_6). Given in Fig. 7 are the system responses obtained by implementing the DAC approach with a discrete-time EKF on the wing rock example using two different process noise covariance values. The results shown in Fig. 7 indicate that the closed-loop system is unstable if the process noise covariance is selected to be 1.00×10^{-15}. The overall system performance is very similar to the desired performance if the process noise covariance is selected to be 1.00×10^{15}.

The estimated disturbances for both process noise covariance values are given in Fig. 8(a). The estimated disturbance is highly noisy if the process noise covariance is selected to be 1.00×10^{15}. The control inputs are shown in Fig. 8(b). The control input for process noise covariance, $Q = 1.00 \times 10^{15}$, is highly noisy. On the other hand, the control input for process noise covariance, $Q = 1.00 \times 10^{-15}$, is noise free but it is much different from the nominal control input.

D. Simulation Results for Case 4

In case 4, the DAC approach with a discrete-time EKF is implemented on a system where the disturbance is induced by a decrease in the input value (c_6). Figure 9 compares the system responses obtained from the DAC approach with a discrete-time EKF to the desired response for two different process noise covariance

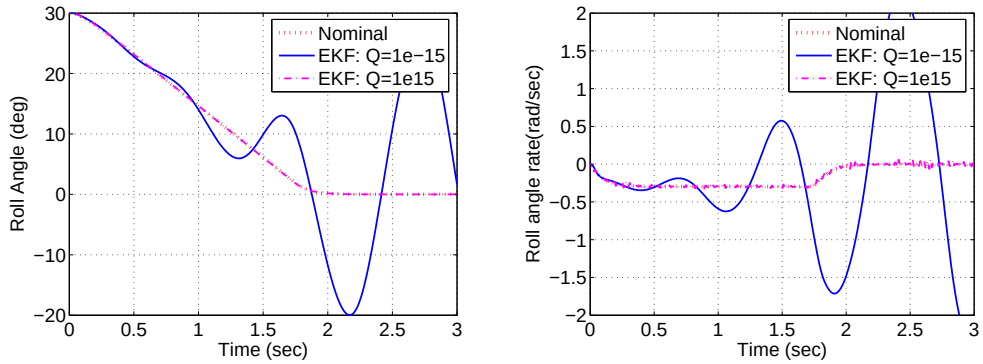

(a) System Response(Roll Angle) (b) System Response(Roll Angle rate)

Figure 7. System Response for Case 3.

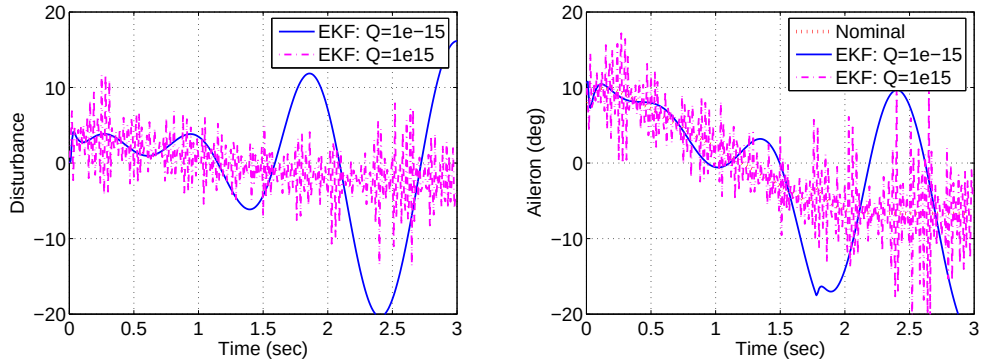

(a) Disturbance (b) Control Input

Figure 8. Disturbance and Control Input for Case 3.

values. Figures 9(a) and 9(b) indicates that the the closed-loop system is unstable if the process noise covariance is selected to be 1.00×10^{-15}.

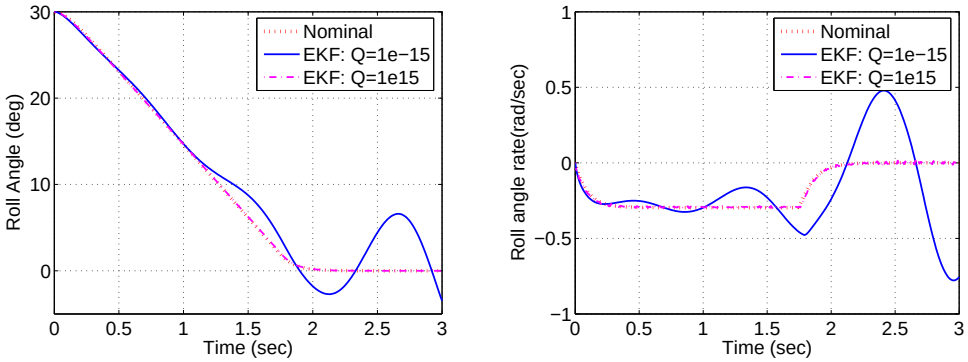

(a) System Response(Roll Angle) (b) System Response(Roll Angle rate)

Figure 9. System Response for Case 4.

The estimated disturbances for both process noise covariance values are given in Fig. 10(a). The results indicate that the estimated disturbance is highly noisy if the process noise covariance is selected to be 1.00×10^{15}. The control inputs or the aileron deflections are shown in Fig. 10(b). The control input for process noise covariance, $Q = 1.00 \times 10^{15}$, is highly noisy. The control input for process noise covariance, $Q = 1.00 \times 10^{-15}$, is noise free but it is much different from the nominal control input.

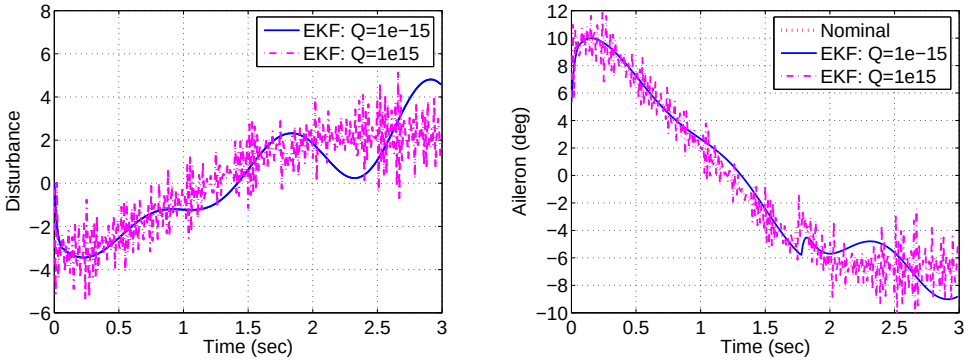

(a) Disturbance (b) Control Input

Figure 10. Disturbance and Control Input for Case 4.

E. Simulation Results for Case 5

Given in Fig. 11 are the system response obtained by implementing the DAC approach with single EKF on the wing rock example using two different process noise covariance values for case 5. The results shown in Fig. 11 indicate that the closed-loop system is unstable if the process noise covariance is selected to be 1.00×10^{-15}. The overall system performance is very similar to the desired performance if the process noise covariance is selected to be 1.00×10^{15}.

The estimated disturbances for both process noise covariance values are given in Fig. 12(a). The estimated disturbance is highly noisy if the process noise covariance is selected to be 1.00×10^{15}. The control inputs or the aileron deflections are shown in Fig. 12(b). The control input for process noise covariance, $Q = 1.00 \times 10^{15}$, is highly noisy.

The simulation results obtained for all five disturbance scenarios indicate that the close-loop system is unstable for small values of process noise covariance. The results also indicate that the DAC approach with a discrete-time EKF approach results in a desired roll-angle response but noisy disturbance estimation and control input if the process noise covariance is selected to be 1.00×10^{15}, which corresponds to the minimum

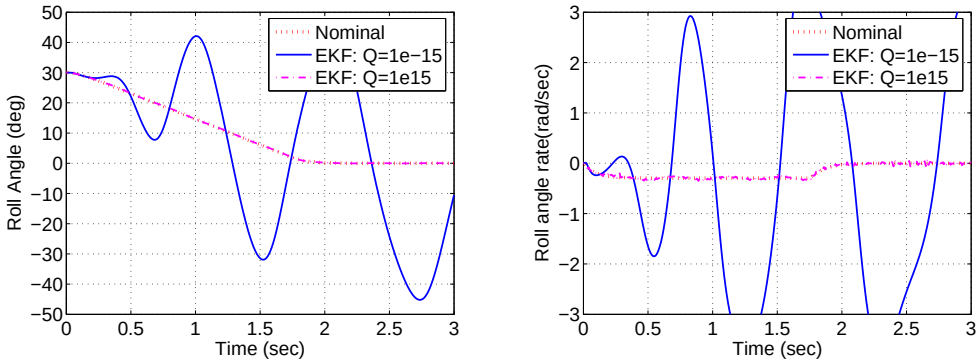

(a) System Response(Roll Angle) (b) System Response(Roll Angle rate)

Figure 11. System Response for Case 5.

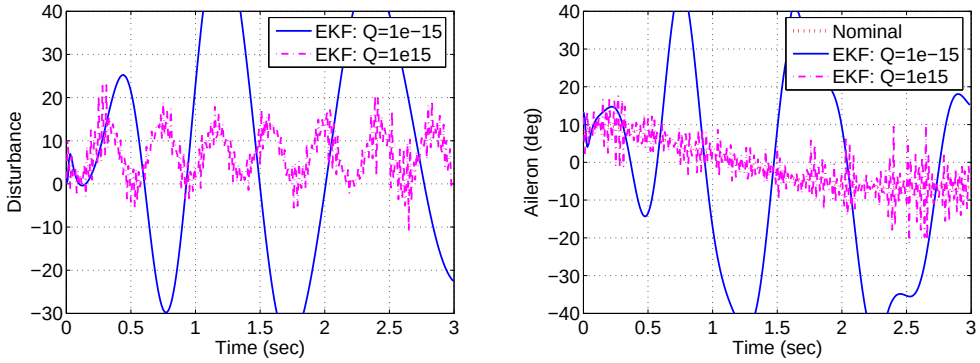

(a) Disturbance (b) Control Input

Figure 12. Disturbance and Control Input for Case 5.

error norm. This clearly shows that the performance of the DAC approach with a discrete-time EKF depends on the process noise covariance value and best performance is obtained when the covariance is tuned to an optimal value.

F. Simulation Results using Optimal Process Noise Covariance Value

From trial and error, the optimal process noise covariance value is selected to be 10.00 for all cases except for case 1. For case 1, the optimal process noise covariance is selected to be 1.00. Given in Fig. 13 are the simulation results obtained from the DAC approach with a discrete-time EKF using the optimal process noise covariance for no disturbance scenario. Figure 13(a) indicates that the system response obtained is identical to the desired response and the control input shown in Fig. 13(b) is noise free. In order to further analyze the results obtained from the DAC approach with a discrete-time EKF, a Monte Carlo simulation is implemented using the optimal process noise covariance value. The results of the Monte Carlo simulations are given in Table 2. The results indicate that the average error norm attained from implementing the DAC approach with a discrete-time EKF is 0.0493 for the no disturbance case.

Given in Fig. 14 are the simulation results obtained using the DAC approach with a discrete-time EKF with the optimal process noise covariance for case 2. Figure 14(a) indicates that the system roll-angle response obtained is identical to the desired response and the control input shown in Fig. 14(b) is noise free. The estimated disturbance shown in Fig. 14(c) is also noise free.

Figures 15, 16, and 17 contain the simulation results obtained from the DAC approach with a discrete-time EKF using the optimal process noise covariance for the disturbance scenarios 3, 4, and 5, respectively. Figures 15(a), 16(a), and 17(a) indicate that the system responses obtained are identical to the desired response.

Table 2. Monte Carlo Simulation Results: Process Noise Covariance vs. Error Norm

Case 1 $Q = 1.0 \times 10^{0}$	**Case 2** $Q = 1.0 \times 10^{01}$	**Case 3** $Q = 1.0 \times 10^{01}$	**Case 4** $Q = 1.0 \times 10^{01}$	**Case 5** $Q = 1.0 \times 10^{01}$
0.0654	5.2964	1.1622	1.9639	3.8849
0.0267	5.3098	1.1671	1.9584	3.8593
0.0597	5.3368	1.1769	2.0203	3.8323
0.0472	5.3067	1.1887	1.9446	3.8800
0.0403	5.3170	1.1464	2.0157	3.9276
0.0949	5.3039	1.1804	1.9590	3.8313
0.0393	5.3224	1.1730	1.9687	3.8665
0.0693	5.3226	1.1735	1.9257	3.8457
0.0363	5.3431	1.1571	1.9666	3.8720
0.0340	5.3293	1.1755	1.9608	3.8408
0.0403	5.3178	1.1774	1.9371	3.8409
0.0254	5.3074	1.1405	1.9490	3.8331
0.0655	5.3365	1.1765	1.9745	3.8194
0.0352	5.2900	1.1563	1.9378	3.8548
0.0466	5.2899	1.1706	1.9394	3.8797
0.0530	5.3383	1.1612	1.9777	3.8912
0.0487	5.2674	1.1602	1.9727	3.8517
0.0836	5.3543	1.1364	1.9269	3.8508
0.0387	5.3106	1.1460	1.9711	3.8604
0.0324	5.3604	1.1520	1.9213	3.8397
0.0534	5.3220	1.1640	1.9070	3.8849
0.0813	5.3198	1.2066	1.9355	3.8883
0.0512	5.2755	1.2239	2.0173	3.8947
0.0221	5.3077	1.1922	2.0037	3.8757
0.0410	5.3303	1.1617	1.9824	3.8750
Avg: 0.0493	Avg: 5.3166	Avg: 1.1691	Avg: 1.9615	Avg: 3.8632

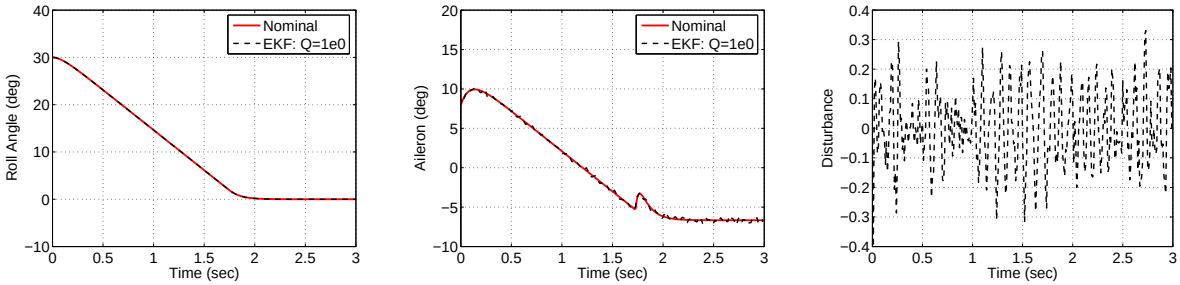

(a) Roll-Angle (b) Aileron Deflection (c) Estimated Disturbance

Figure 13. Case 1: System Response, Control Input, and Estimated Disturbance for $\mathbf{Q} = 1.00 \times 10^{+00}$

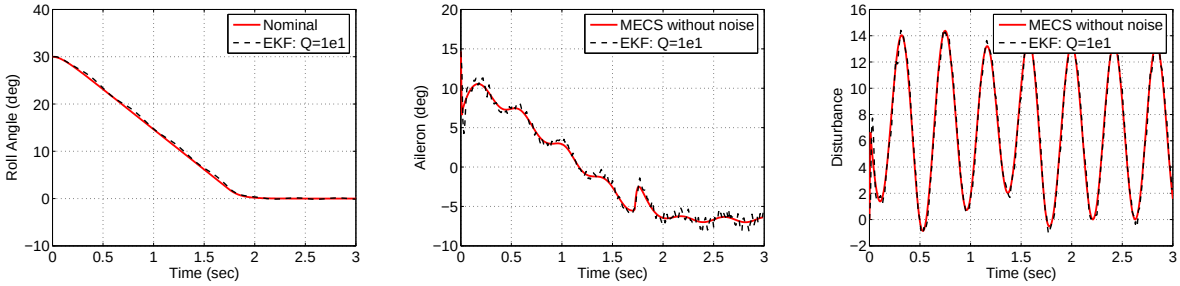

(a) Roll-Angle (b) Aileron Deflection (c) Estimated Disturbance

Figure 14. Case 2: System Response, Control Input, and Estimated Disturbance for $\mathbf{Q} = 1.00 \times 10^{+01}$

The control input signals obtained are without noise. The estimated disturbance shown in Fig. 15(c), 16(c), and 17(c) are also noise free.

The simulation results obtained for all five disturbance scenarios indicate that the closed-loop system is unstable for small values of process noise covariance. This due to the fact that when a small process noise covariance value is selected, the EKF assumes there is no uncertainties associated with the assumed system model and the disturbance accommodating controller reduce down to just the nominal controller. The results also indicate that the DAC approach with a discrete-time EKF results in the desired roll-angle response but noisy disturbance estimation and control input if the process noise covariance is selected to be 1.00×10^{15}. Selecting a very large process noise covariance value will compel the EKF to completely rely upon the measurement signal and therefore the noise associated with the measurement signal directly gets transmitted to the estimates. There results clearly illustrate that the performance of the DAC approach with a discrete-time EKF depends on the process noise covariance value and the best performance is obtained

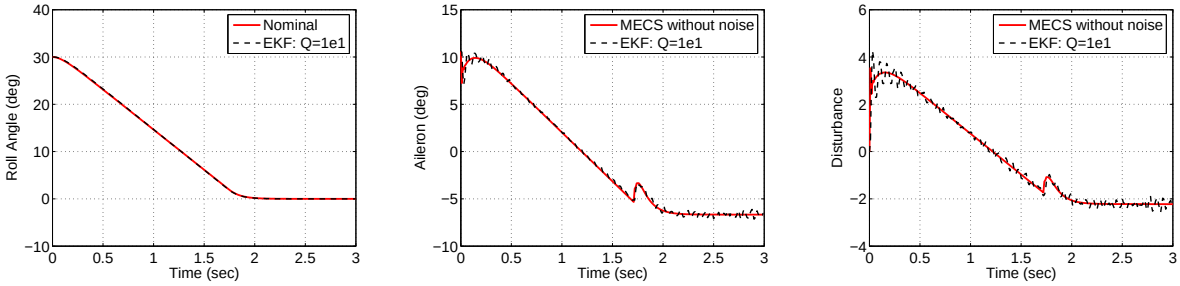

(a) Roll-Angle (b) Aileron Deflection (c) Estimated Disturbance

Figure 15. Case 3: System Response, Control Input, and Estimated Disturbance for $\mathbf{Q} = 1.00 \times 10^{+01}$

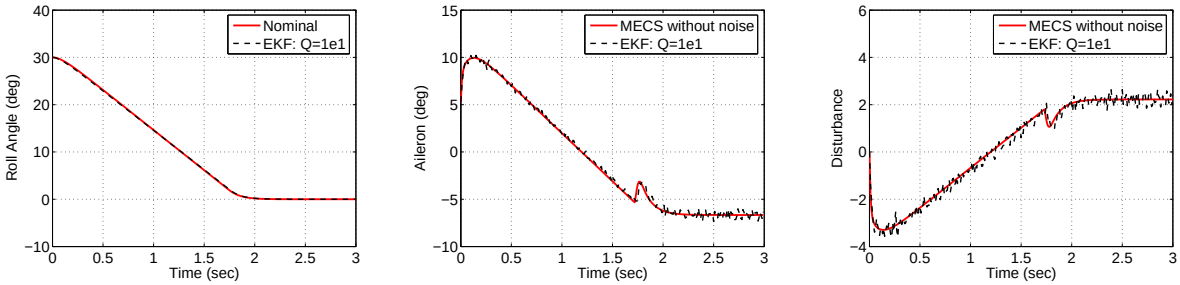

(a) Roll-Angle (b) Aileron Deflection (c) Estimated Disturbance

Figure 16. Case 4: System Response, Control Input, and Estimated Disturbance for Q = $1.00 \times 10^{+01}$

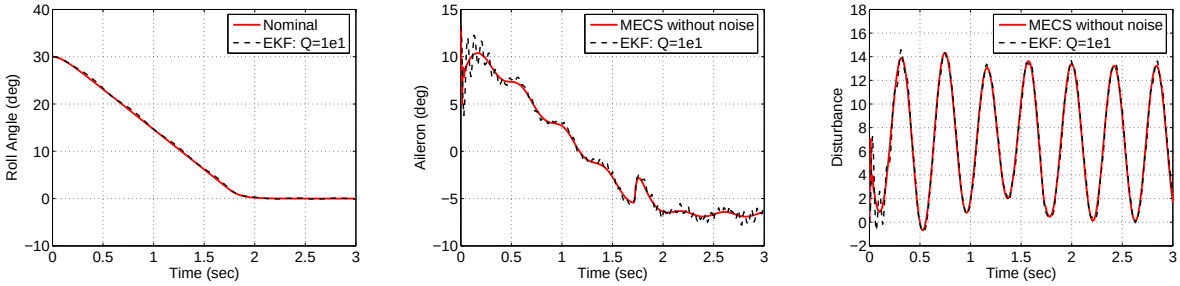

(a) Roll-Angle (b) Aileron Deflection (c) Estimated Disturbance

Figure 17. Case 5: System Response, Control Input, and Estimated Disturbance for Q = $1.00 \times 10^{+01}$

when the covariance is tuned to an optimal value. Notice that the optimal process noise covariance value is indicative of how well one knows the uncertainties and the external disturbance associated with the system. The simulation results also indicate that after tuning the process noise covariance value to 10.00, the DAC approach with a discrete-time EKF successfully estimates the disturbance even in the presence of noise. The main disadvantage of using the EKF in the DAC approach for disturbance prediction is that the stability of closed-loop system depends on the process noise covariance value. To further investigate the influence of process noise covariance on the stability, a closed-loop Lyapunov stability analysis is conducted in next section.

V. Lyapunov Stability Analysis

Simulation results shown in previous section indicate that the stability of a closed-loop system utilizing DAC approach with discrete-time EKF depends on the process noise covariance value. In order to further investigate this phenomenon, a Lyapunov stability analysis is conducted on a linear system which uses the DAC approach with linear continuous-time Kalman filter.

Consider a simple first order system of the following form

$$\begin{aligned} \dot{x} &= ax + bu + w \\ y &= cx + v \end{aligned} \tag{28}$$

where x is the system state, u is the control input and y represents the system output. The variables w and v represent the external disturbance and the measurement noise, respectively. They are assumed to be independent of each other, zero-mean, white and with normal probability distribution, i.e.

$$\begin{aligned} p(w) &\sim N(0, q), \\ p(v) &\sim N(0, r) \end{aligned} \tag{29}$$

The assumed model of the above system is

$$\begin{aligned} \dot{x}_m &= a_m x_m + b_m u + d_m \\ y_m &= c x_m + v \end{aligned} \tag{30}$$

where a_m and b_m are assumed system parameters. The disturbance term, d_m, compensate for the external disturbance and the model uncertainties, i.e.

$$d_m = (a - a_m)x_m + (b - b_m)u + w \tag{31}$$

Now construct an extended state vector, $\mathbf{z}_m = [x_m \quad d_m]^T$, and assume zero dynamics for the disturbance term, i.e.

$$\begin{bmatrix} \dot{x}_m \\ \dot{d}_m \end{bmatrix} = \begin{bmatrix} a_m & 1 \\ 0 & 0 \end{bmatrix} \begin{bmatrix} x_m \\ d_m \end{bmatrix} + \begin{bmatrix} b_m \\ 0 \end{bmatrix} u + \begin{bmatrix} 0 \\ \sigma \end{bmatrix} \tag{32}$$

where σ is assumed to be zero mean white noise associated with the disturbance process. The above equation, Eq. (32), can be written in terms of the appended state vector, $\mathbf{z}_m$, as

$$\dot{\mathbf{z}}_m = F_m \mathbf{z}_m + B_m u + \mathbf{w}_m \tag{33}$$

The assumed output equation can also be written in terms of the appended state vector, $\mathbf{z}_m$, as

$$y_m = \begin{bmatrix} c & 0 \end{bmatrix} \mathbf{z}_m + v \tag{34}$$

Now append the disturbance term, d_m, to the true system state, x, and let $\mathbf{z} = [x \quad d_m]^T$. The true system equation, Eq. (28), can be written in terms of the appended state vector, $\mathbf{z}$, as

$$\begin{bmatrix} \dot{x} \\ \dot{d}_m \end{bmatrix} = \begin{bmatrix} a & 0 \\ 0 & 0 \end{bmatrix} \begin{bmatrix} x \\ d_m \end{bmatrix} + \begin{bmatrix} b \\ 0 \end{bmatrix} u + \begin{bmatrix} w \\ \sigma \end{bmatrix} \tag{35}$$

or in more compact form as

$$\dot{\mathbf{z}} = F\mathbf{z} + Bu + \mathbf{w} \tag{36}$$

The measured output equation can be written as

$$y = \begin{bmatrix} c & 0 \end{bmatrix} \mathbf{z} + v \tag{37}$$

Though the disturbance term in unknown, assuming the process noise, $\mathbf{w}_m$, and the measurement noise, v, possess certain stochastic properties, an optimal estimator such as a Kalman filter can be implemented in the feedback loop to estimate the system state and the disturbance term from the noisy measurements. The estimator dynamics can be written as

$$\dot{\hat{\mathbf{z}}} = F_m \hat{\mathbf{z}} + B_m u + K[y - \hat{y}] \tag{38}$$

where K is the Kalman gain and $\hat{y} = c\hat{x}$ is the estimated output. Let $H = [c \ 0]$, then $y = H\mathbf{z} + v$ and $\hat{y} = H\hat{\mathbf{z}}$. Now the estimator can be rewritten as

$$\dot{\hat{\mathbf{z}}} = F_m \hat{\mathbf{z}} + B_m u + KH[\mathbf{z} - \hat{\mathbf{z}}] + \mathbf{v} \tag{39}$$

The control objective is to obtain asymptotic stability for the plant, and it is possible by implementing a control law of the form

$$\begin{aligned} u &= \begin{bmatrix} -k_m & -\dfrac{1}{b_m} \end{bmatrix} \begin{bmatrix} \hat{x} \\ \hat{d}_m \end{bmatrix} \\ &= S\hat{\mathbf{z}} \end{aligned} \tag{40}$$

where k_m is the feedback gain and $k_m > a_m$. While the feedback gain, k_m, guarantees that the system is asymptotically stable, the second gain, $\frac{1}{b_m}$, ensures the complete cancelation of the disturbance term which is compensating for the external disturbance and the model uncertainties.

After substituting the control law, Eq. (40), into the plant dynamics, Eqs. (36) and (39) can be written as

$$\dot{\mathbf{z}} = F\mathbf{z} + BS\hat{\mathbf{z}} + \mathbf{w} \tag{41}$$

$$\dot{\hat{\mathbf{z}}} = F_m\hat{\mathbf{z}} + B_mS\hat{\mathbf{z}} + KH[\mathbf{z} - \hat{\mathbf{z}}] + \mathbf{v} \tag{42}$$

Let $\tilde{\mathbf{z}} = \mathbf{z} - \hat{\mathbf{z}}$, then the asymptotic stability of this control scheme is assured if $\tilde{\mathbf{z}}$ asymptotically approaches zero, i.e., $\lim_{t\to\infty} \tilde{\mathbf{z}}(t) = 0$. The error dynamics is defined as

$$\begin{aligned}
\dot{\tilde{\mathbf{z}}} &= \dot{\mathbf{z}} - \dot{\hat{\mathbf{z}}} \\
&= F\mathbf{z} + BS\hat{\mathbf{z}} + \mathbf{w} - F_m\hat{\mathbf{z}} - B_mS\hat{\mathbf{z}} - KH[\mathbf{z} - \hat{\mathbf{z}}] - \mathbf{v} \\
&= (F - F_m)\mathbf{z} + F_m(\mathbf{z} - \hat{\mathbf{z}}) + (B - Bm)S\hat{\mathbf{z}} - KH[\mathbf{z} - \hat{\mathbf{z}}] + \mathbf{w} - \mathbf{v} \\
&= \triangle F\mathbf{z} + F_m\tilde{\mathbf{z}} + \triangle BS\hat{\mathbf{z}} - KH\tilde{\mathbf{z}} + \mathbf{w} - \mathbf{v}
\end{aligned}$$

Without lose of generality, the two zero mean white nose terms $\mathbf{w}$ and $\mathbf{v}$ can be combined into one term, $\boldsymbol{\nu}$. After substituting for the Kalman gain, $K = PH^TR^{-1}$, the error dynamics can be rewritten as

$$\dot{\tilde{\mathbf{z}}} = [F_m - PH^TR^{-1}H]\tilde{\mathbf{z}} + \triangle F\mathbf{z} + \triangle BS\hat{\mathbf{z}} + \boldsymbol{\nu} \tag{43}$$

the matrix P is the error covariance matrix and the covariance equation for a linear continuous-time Kalman filter is

$$P(t) = F_mP(t) + P(t){F_m}^T - P(t)H^TR^{-1}HP(t) + Q \tag{44}$$

where R is the measurement noise covariance and Q is the process noise covariance, i.e.

$$\begin{aligned}
p(\mathbf{w}) &\sim N(0, Q), \\
p(\mathbf{v}) &\sim N(0, R)
\end{aligned} \tag{45}$$

Now consider the following candidate Lyapunov function:

$$V[\tilde{\mathbf{z}}(t)] = \tilde{\mathbf{z}}^T(t)P^{-1}(t)\tilde{\mathbf{z}}(t) \tag{46}$$

Since $P(t)P^{-1}(t) = I$, the time derivative of $P(t)P^{-1}(t)$ is 0, i.e.

$$\frac{d}{dt}\Big[P(t)P^{-1}(t)\Big] = \dot{P}(t)P^{-1}(t) + P(t)\dot{P}^{-1}(t) = 0 \tag{47}$$

Solving the above equation for $\dot{P}^{-1}(t)$ gives

$$\dot{P}^{-1}(t) = -P^{-1}(t)\dot{P}(t)P^{-1}(t) \tag{48}$$

$$= -P^{-1}(t)F_m - F_m^TP^{-1}(t) + H^TR^{-1}H - P^{-1}(t)QP^{-1}(t) \tag{49}$$

Now the time derivative of Eq. (46) can be written as

$$\begin{aligned}
\dot{V}[\tilde{\mathbf{z}}(t)] &= \dot{\tilde{\mathbf{z}}}^TP^{-1}\tilde{\mathbf{z}} + \tilde{\mathbf{z}}^T\dot{P}^{-1}\tilde{\mathbf{z}} + \tilde{\mathbf{z}}^TP^{-1}\dot{\tilde{\mathbf{z}}} \\
&= 2\tilde{\mathbf{z}}^TP^{-1}\dot{\tilde{\mathbf{z}}} + \tilde{\mathbf{z}}^T\dot{P}^{-1}\tilde{\mathbf{z}} \\
&= 2\tilde{\mathbf{z}}^TP^{-1}\Big[[F_m - PH^TR^{-1}H]\tilde{\mathbf{z}} + \triangle F\mathbf{z} + \triangle BS\hat{\mathbf{z}} + \boldsymbol{\nu}\Big] + \\
&\quad \tilde{\mathbf{z}}^T\Big[- P^{-1}(t)F_m - F_m^TP^{-1}(t) + H^TR^{-1}H - P^{-1}(t)QP^{-1}(t)\Big]\tilde{\mathbf{z}}
\end{aligned}$$

After some algebraic manipulations, $\dot{V}[\tilde{\mathbf{z}}(t)]$ can be written as

$$\dot{V}[\tilde{\mathbf{z}}(t)] = -\tilde{\mathbf{z}}^TH^TR^{-1}H\tilde{\mathbf{z}} + 2\tilde{\mathbf{z}}^TP^{-1}\triangle F\mathbf{z} + 2\tilde{\mathbf{z}}^TP^{-1}\triangle BS\hat{\mathbf{z}} + 2\tilde{\mathbf{z}}^TP^{-1}\boldsymbol{\nu} - \tilde{\mathbf{z}}^TP^{-1}QP^{-1}\tilde{\mathbf{z}} \tag{50}$$

For asymptotic stability $\dot{V}[\tilde{\mathbf{z}}(t)]$ must be negative definite. Notice that the terms $\tilde{\mathbf{z}}^T H^T R^{-1} H\tilde{\mathbf{z}}$ and $\tilde{\mathbf{z}}^T P^{-1} Q P^{-1}\tilde{\mathbf{z}}$ are positive definite. In reality, the measurement noise covariance, R, can easily be determined based on the sensor accuracies. Now if the process noise covariance, Q, selected so that $\tilde{\mathbf{z}}^T P^{-1} Q P^{-1}\tilde{\mathbf{z}}$ can compensate for all the positive terms in Eq. (50), then $\dot{V}[\tilde{\mathbf{z}}(t)]$ is guaranteed to be negative definite. That is, in order for $\dot{V}[\tilde{\mathbf{z}}(t)]$ to be strictly negative, the following inequality must hold.

$$2\tilde{\mathbf{z}}^T P^{-1}\triangle F\mathbf{z} + 2\tilde{\mathbf{z}}^T P^{-1}\triangle BS\hat{\mathbf{z}} + 2\tilde{\mathbf{z}}^T P^{-1}\boldsymbol{\nu} \leq \tilde{\mathbf{z}}^T P^{-1} Q P^{-1}\tilde{\mathbf{z}} \tag{51}$$

The above inequality can be written in a more stricter form as

$$2\|\tilde{\mathbf{z}}^T P^{-1}\triangle F\mathbf{z} + \tilde{\mathbf{z}}^T P^{-1}\triangle BS\hat{\mathbf{z}} + \tilde{\mathbf{z}}^T P^{-1}\boldsymbol{\nu}\| \leq \|\tilde{\mathbf{z}}^T P^{-1} Q P^{-1}\tilde{\mathbf{z}}\| \tag{52}$$

Using the triangle inequality, the LHS of Eq. (52) can be written as

$$\begin{aligned} 2\|\tilde{\mathbf{z}}^T P^{-1}\triangle F\mathbf{z} + \tilde{\mathbf{z}}^T P^{-1}\triangle BS\hat{\mathbf{z}} + \tilde{\mathbf{z}}^T P^{-1}\boldsymbol{\nu}\| \leq 2\|\tilde{\mathbf{z}}^T\|\|P^{-1}\|\|\triangle F\|\|\mathbf{z}\| + \\ 2\|\tilde{\mathbf{z}}^T\|\|P^{-1}\|\|\triangle B\|\|S\|\|\hat{\mathbf{z}}\| + 2\|\tilde{\mathbf{z}}^T\|\|P^{-1}\|\|\boldsymbol{\nu}\| \end{aligned} \tag{53}$$

Also the RHS of Eq. (52) can be written as

$$\|\tilde{\mathbf{z}}^T P^{-1} Q P^{-1}\tilde{\mathbf{z}}\| \leq \|\tilde{\mathbf{z}}^T\|\|P^{-1}\|\|Q\|\|P^{-1}\|\|\tilde{\mathbf{z}}\| \tag{54}$$

Notice that if Eq. (52) is true, then the following inequality holds

$$\begin{aligned} 2\|\tilde{\mathbf{z}}^T\|\|P^{-1}\|\|\triangle F\|\|\mathbf{z}\| + 2\|\tilde{\mathbf{z}}^T\|\|P^{-1}\|\|\triangle B\|\|S\|\|\hat{\mathbf{z}}\| + 2\|\tilde{\mathbf{z}}^T\|\|P^{-1}\|\|\boldsymbol{\nu}\| \leq \\ \|\tilde{\mathbf{z}}^T\|\|P^{-1}\|\|Q\|\|P^{-1}\|\|\tilde{\mathbf{z}}\| \end{aligned} \tag{55}$$

Equation (55) can be rewritten as

$$2\|\triangle F\|\|\mathbf{z}\| + 2\|\triangle B\|\|S\|\|\hat{\mathbf{z}}\| + 2\|\boldsymbol{\nu}\| \leq \|Q\|\|P^{-1}\|\|\tilde{\mathbf{z}}\| \tag{56}$$

From Eq. (56), the necessary condition for the asymptotic stability of the disturbance accommodation control strategy with Kalman filter can be expressed as

$$\|Q\| \geq \Big[2\|\triangle F\|\|\mathbf{z}\| + 2\|\triangle B\|\|S\|\|\hat{\mathbf{z}}\| + 2\|\boldsymbol{\nu}\|\Big](\|P^{-1}\|\|\tilde{\mathbf{z}}\|)^{-1} \tag{57}$$

Notice that if there is no model uncertainties, external disturbance and measurement noise, then $\|\triangle F\| = \|\triangle B\| = \|\boldsymbol{\nu}\| = 0$ and the above inequality reduce down to $\|Q\| \geq 0$.

VI. Verification of Lyapunov Analysis

A detailed investigation of the above Lyapunov stability proof through numerical simulation is given in this section. First the nonlinear wing-rock system given in Eqs. (14) and (15) is simplified into the following linear system

$$\begin{bmatrix}\dot{\phi}\\ \dot{p}\end{bmatrix} = \begin{bmatrix}0 & 1\\ c_2 & c_3\end{bmatrix}\begin{bmatrix}\phi\\ p\end{bmatrix} + \begin{bmatrix}0\\ c_6\end{bmatrix} u \tag{58}$$

Notice that for simplicity, external disturbance is not considered here. The assumed model of the above system is given as

$$\begin{bmatrix}\dot{\phi}_m\\ \dot{p}_m\end{bmatrix} = \begin{bmatrix}0 & 1\\ \bar{c}_2 & \bar{c}_3\end{bmatrix}\begin{bmatrix}\phi_m\\ p_m\end{bmatrix} + \begin{bmatrix}0\\ \bar{c}_6\end{bmatrix} u + \begin{bmatrix}0\\ d_m\end{bmatrix} \tag{59}$$

In order to be consistent with previous notations, the assumed system parameters are indicated as $\bar{c}_2$, $\bar{c}_3$, and $\bar{c}_6$. Suppose there is no measurement noise, now the true measurement and the assumed measurement equations are given as

$$y = \phi \tag{60}$$

$$y_m = \phi_m \tag{61}$$

Let the extended state vector, $\mathbf{z}_m = [\phi_m \quad p_m \quad d_m]^T$, now the assumed extended system equation can be written as

$$\begin{bmatrix} \dot{\phi}_m \\ \dot{p}_m \\ \dot{d}_m \end{bmatrix} = \begin{bmatrix} 0 & 1 & 0 \\ \bar{c}_2 & \bar{c}_3 & 1 \\ 0 & 0 & 0 \end{bmatrix} \begin{bmatrix} \phi_m \\ p_m \\ d_m \end{bmatrix} + \begin{bmatrix} 0 \\ \bar{c}_6 \\ 0 \end{bmatrix} u + \begin{bmatrix} 0 \\ 0 \\ \sigma \end{bmatrix} \tag{62}$$

where σ, the noise associated with the disturbance process, assumed to have the following stochastic properties

$$p(\sigma) \sim N(0, q), \tag{63}$$

Equation (62), can be written in terms of the appended state vector, $\mathbf{z}_m$, as

$$\dot{\mathbf{z}}_m = F_m \mathbf{z}_m + B_m u + G\sigma \tag{64}$$

Now append the disturbance term, d_m, to the true system states and let $\mathbf{z} = [\phi \quad p \quad d_m]^T$. The true system equation, Eq. (58), can be written in terms of the appended state vector, $\mathbf{z}$, as

$$\begin{bmatrix} \dot{\phi} \\ \dot{p} \\ \dot{d}_m \end{bmatrix} = \begin{bmatrix} 0 & 1 & 0 \\ c_2 & c_3 & 0 \\ 0 & 0 & 0 \end{bmatrix} \begin{bmatrix} \phi \\ p \\ d_m \end{bmatrix} + \begin{bmatrix} 0 \\ c_6 \\ 0 \end{bmatrix} u + \begin{bmatrix} 0 \\ 0 \\ \sigma \end{bmatrix} \tag{65}$$

or in more compact form as

$$\dot{\mathbf{z}} = F\mathbf{z} + Bu + G\sigma \tag{66}$$

The measured output equation can be written as

$$y = \begin{bmatrix} 1 & 0 & 0 \end{bmatrix} \mathbf{z} \tag{67}$$

The estimator equation can be written as

$$\dot{\hat{\mathbf{z}}} = F_m \hat{\mathbf{z}} + B_m u + KH[\mathbf{z} - \hat{\mathbf{z}}] \tag{68}$$

where K is the Kalman gain and $H = [1 \;\; 0 \;\; 0]$. Notice that after linearizing, the variable structure controller can be reduced down to a simple PD controller of the form

$$\bar{u} = \begin{bmatrix} k_p & k_d \end{bmatrix} \begin{bmatrix} \hat{\phi} \\ \hat{p} \end{bmatrix} \tag{69}$$

where

$$k_p = -\frac{\bar{c}_2}{\bar{c}_6} - \frac{\vartheta\eta}{\rho\bar{c}_6}$$

and

$$k_d = \frac{\bar{c}_3}{\bar{c}_6} + \frac{\vartheta}{\bar{c}_6} + \frac{\eta}{\rho\bar{c}_6}$$

The total control input, which include the nominal controller together with the control correction can be expressed as

$$u = \begin{bmatrix} k_p & k_d & -\frac{1}{\bar{c}_6} \end{bmatrix} \begin{bmatrix} \hat{\phi} \\ \hat{p} \\ \hat{d}_m \end{bmatrix} = S\hat{\mathbf{z}} \tag{70}$$

After substituting the control law into Eqs. (66) and (68), the closed-loop system in state-space can be written as

$$\begin{bmatrix} \dot{\phi} \\ \dot{p} \\ \dot{\hat{\phi}} \\ \dot{\hat{p}} \\ \dot{\hat{d}}_m \end{bmatrix} = \begin{bmatrix} 0 & 1 & 0 & 0 & 0 \\ c_2 & c_3 & c_6 k_p & c_6 k_d & -\frac{c_6}{\bar{c}_6} \\ k_1 & 0 & -k_1 & 1 & 0 \\ k_2 & 0 & \bar{c}_2 + \bar{c}_6 k_p - k_2 & \bar{c}_3 + \bar{c}_6 k_d & -1 \\ k_3 & 0 & -k_3 & 0 & 0 \end{bmatrix} \begin{bmatrix} \phi \\ p \\ \hat{\phi} \\ \hat{p} \\ \hat{d}_m \end{bmatrix} \tag{71}$$

Note that the closed-loop system given above is time varying since the Kalman gain, $K = [k_1 \;\; k_2 \;\; k_3]^T$, is time varying. Calculation of the Kalman gain requires the propagation of the 3×3 error covariance matrix, $P(t)$, using the continuous-time matrix differential Riccati equation given in Eq. (44). Fortunately, since the system given in Eq. (66) is time-invariant, the error covariance, $P(t)$, reaches a steady-state value very quickly. This steady state $P(t)$ is the solution to the continuous-time matrix algebraic Riccati equation given below:

$$F_m P + P {F_m}^T - P H^T R^{-1} H P + Q = 0 \tag{72}$$

Now the steady state Kalman gain can be calculated using the equation $K = PH^T R^{-1}$. If the time-varying gain in Eq. (71) is replaced with the steady-state gain, then the resulting system is time-invariant and the stability of this time-invariant system can easily be verified by calculating the closed loop poles.

For simulation purposes, the true system parameters are selected to be

$$c_2 = -26.7, \;\; c_3 = 0.765, \;\; \text{and} \;\; c_6 = 0.75 \tag{73}$$

and the assumed system parameters are

$$\bar{c}_2 = -26.7\beta, \;\; \bar{c}_3 = 0.765\beta, \;\; \text{and} \;\; \bar{c}_6 = 0.75\beta \tag{74}$$

where β is a scalar parameter which introduces uncertainties into the assumed system model. Using the assumed system parameters the feedback controller gain can be calculated as

$$S = \begin{bmatrix} \frac{26.7\beta - 300}{0.75\beta} & \frac{0.765\beta + 40}{0.75\beta} & -\frac{1}{0.75\beta} \end{bmatrix} \tag{75}$$

Since there is no measurement noise, a small value is assigned to the measurement noise covariance, i.e.

$$R = 1.0 \times 10^{-05}$$

The initial conditions are selected to be

$$\begin{bmatrix} \phi \\ p \\ \hat{\phi} \\ \hat{p} \\ \hat{d}_m \end{bmatrix} = \begin{bmatrix} \frac{\pi}{6} \\ 0 \\ \frac{\pi}{6} \\ 0 \\ 0 \end{bmatrix}$$

The scalar variable β is selected to be 2.0, thus the assumed system parameters are twice that of the true system parameters. For the first simulation, the process noise covariance value is selected to be 0.01 and the simulation results are shown in Fig. 18. Figure 18 indicate that the closed-loop system is unstable for selected values of Q and R.

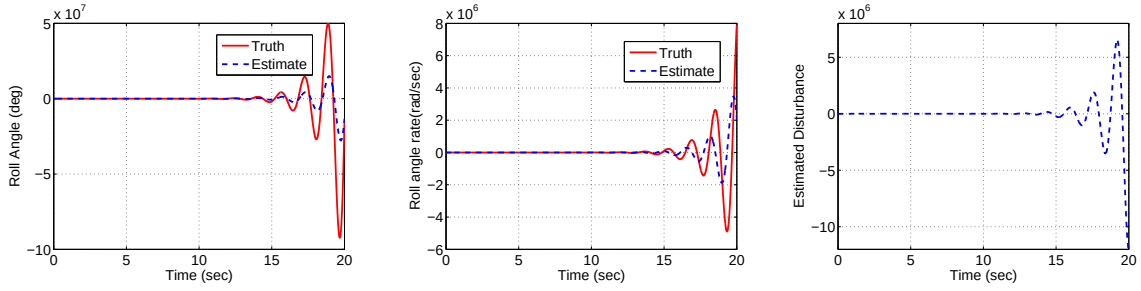

(a) Roll Angle (b) Roll Angle Rate (c) Disturbance

Figure 18. Linear System Response: $Q = 1 \times 10^{-2}$ **and** $R = 1 \times 10^{-5}$

In order to verify whether the results shown in Fig. 18 is consistent with the Lyapunov analysis, the lower bound on the norm of Q required for stability is calculated using Eq. (57) and it is given in Fig. 19(a). Also, the difference between the actual Q norm and the lower bound on Q norm required for stability is calculated, Fig. 19(b). This difference, called the "stability indicator", must be positive at all times in order for the inequality given in Eq. (57) to be true. Figure 19(a) indicates that in order for the inequality given

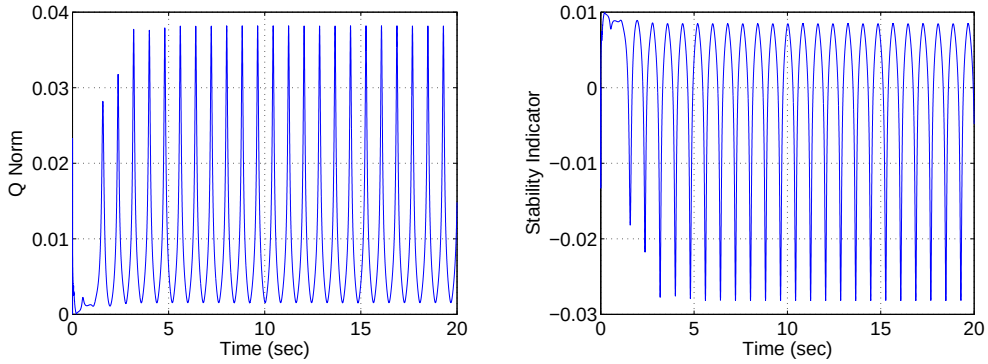

(a) Q Norm required for stability (b) Stability Indicator

Figure 19. Lyapunov Analysis: $Q = 1 \times 10^{-2}$ **and** $R = 1 \times 10^{-5}$

in Eq. (57) to be satisfied, the process noise covariance norm must be greater than 0.04. Since Q is selected to be 0.01, which is less than the required Q norm for stability, the inequality given in Eq. (57) is often violated as indicated by the negative values shown in Fig. 19(b).

A second simulation is conducted using a process noise covariance of 100. System response and the estimated disturbance obtained for the second simulation are shown in Fig. 20. The system roll angle response given in Fig. 20(a) indicates that the given disturbance accommodating control strategy is able to suppress the initial roll angle of 30° within one second. Also note that the system roll angle rate given in Fig. 20(b) and the estimated disturbance given in Fig. 20(c) also vanish after one second.

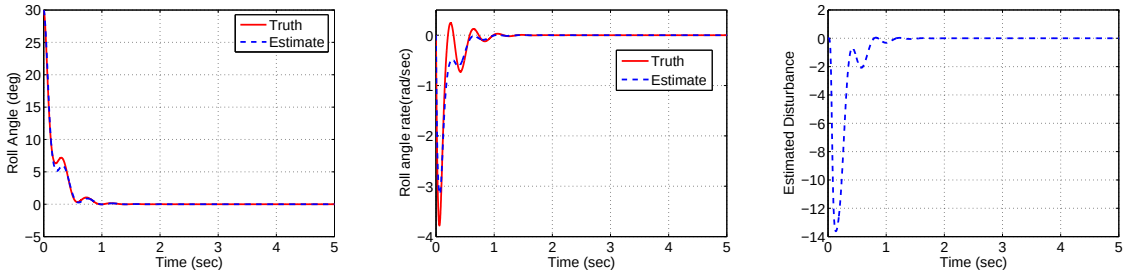

(a) Roll Angle (b) Roll Angle Rate (c) Disturbance

Figure 20. Linear System Response: $Q = 1 \times 10^{2}$ **and** $R = 1 \times 10^{-5}$

Given in Fig. 21 are the lower bound on the norm of Q required for stability and the stability indicator. Figure 21(a) indicates that for Lyapunov stability, the process noise covariance norm must be greater than 2.5. Since Q is selected to be 100, which is greater than the required Q norm for stability, the inequality given in Eq. (57) is always satisfied as indicated by the positive values shown in Fig. 21(b). These simulation results authenticate the validity of the Lyapunov stability analysis shown earlier.

In order to further investigate the sensitivity of the process noise covariance to the closed-loop system stability, additional simulations are conducted using three different measurement noise covariance values, (1.0×10^{-8}, 1.0×10^{-3}, and 1.0×10^{3}). The process noise covariance Q is selected to vary from 1×10^{-10} to $1 \times 10^{+2}$. Based on the Q selected, different steady-state error covariance matrices are calculated using the continuous-time matrix algebraic Riccati equation given in Eq. (72). The steady-state error covariance matrix is then used to calculate the steady-state Kalman gain and the poles of the closed-loop system given in Eq. (71).

Given in Fig. 22 are the system closed-loop poles and the stability indicator for the first simulation where R is selected to be 1.0×10^{-3}. Figure 22(a) shows the migration of the closed-loop system poles from the unstable region to the stable region as Q increases from 1×10^{-10} to $1 \times 10^{+2}$. Given in Fig. 22(b) is the stability indicator which identify the process noise covariance values that do not satisfy the Lyapunov stability requirement given in Eq. (57). Figure 22(b) shows that for process noise covariance values less than

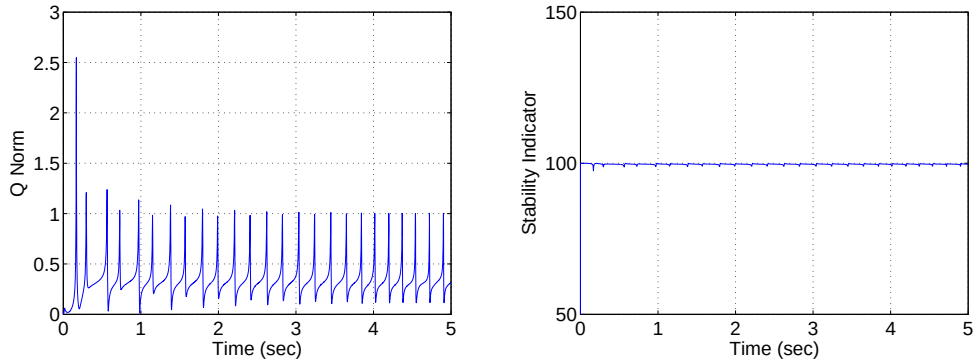

(a) Q Norm required for stability (b) Stability Indicator

Figure 21. Lyapunov Analysis: $Q = 1 \times 10^{2}$ **and** $R = 1 \times 10^{-5}$

1.0, the inequality given in Eq. (57) is violated and therefore the system is unstable as shown in Fig. 22(a).

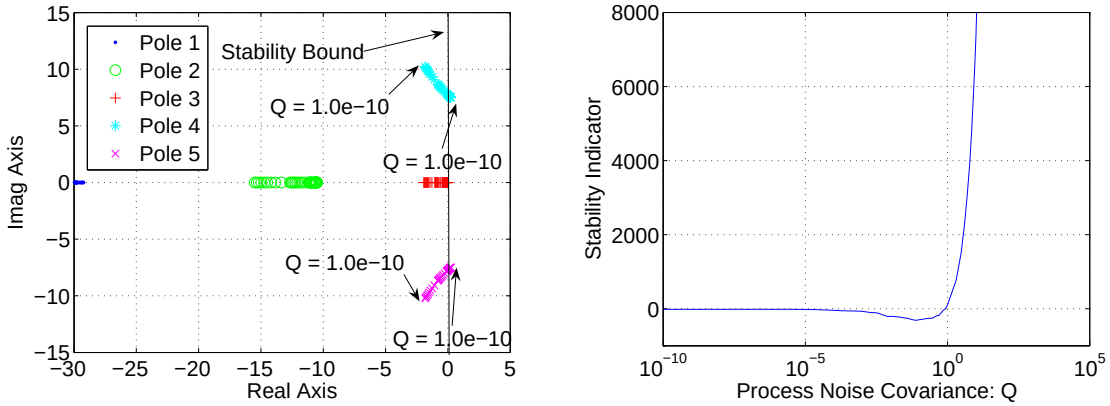

(a) System Closed-Loop Poles (b) Stability Indicator

Figure 22. Closed-Loop Stability Analysis: $Q = [1 \times 10^{-10} \ldots 1 \times 10^{2}]$ **and** $R = 1 \times 10^{-3}$

For the second simulation, the measurement noise covariance value is selected to be 1.0×10^{3}. Given in Fig. 23 are the system closed-loop poles and the stability indicator for the second simulation. Figure 23(a) shows that the closed-loop system is unstable for any values of Q between 1×10^{-10} and $1 \times 10^{+2}$. The consistent negative values given in Fig. 23(b) supports this results. This instability is due to the fact that as R increases, the first term in Eq. (50), $\tilde{\mathbf{z}}^{T} H^{T} R^{-1} H \tilde{\mathbf{z}}$, approaches zero and therefore a large values of Q is required to assure Eq. (50) is negative definite. In order to investigate this phenomenon, more simulations are conducted using the same measurement noise covariance value, but this time Q is selected to vary from 1×10^{5} to 1×10^{8}.

Given in Fig. 24 are the system closed-loop poles and the stability indicator for the simulation where R is selected to be 1.0×10^{-3} and the Q is selected to vary from 1×10^{5} to 1×10^{8}. Figure 24(a) shows the migration of the closed-loop system poles from the unstable region to the stable region as Q increases from 1×10^{5} to 1×10^{8}. Given in Fig. 24(b) is the stability indicator which shows that, for process noise covariance values less than 7×10^{5}, the inequality given in Eq. (57) is violated and therefore the system is unstable as shown in Fig. 24(a).

For the third simulation, the measurement noise covariance value is selected to be 1.0×10^{-8}. Given in Fig. 25 are the system closed-loop poles and the stability indicator for the third simulation. Figure 25(a) shows that the major portion of closed-loop system poles are in stable region. This is consistent with the positive stability indicator values attained for small process noise covariance values as shown in Fig. 25(b).

The numerical simulations shown in this section authenticate the Lyapunov stability analysis given in

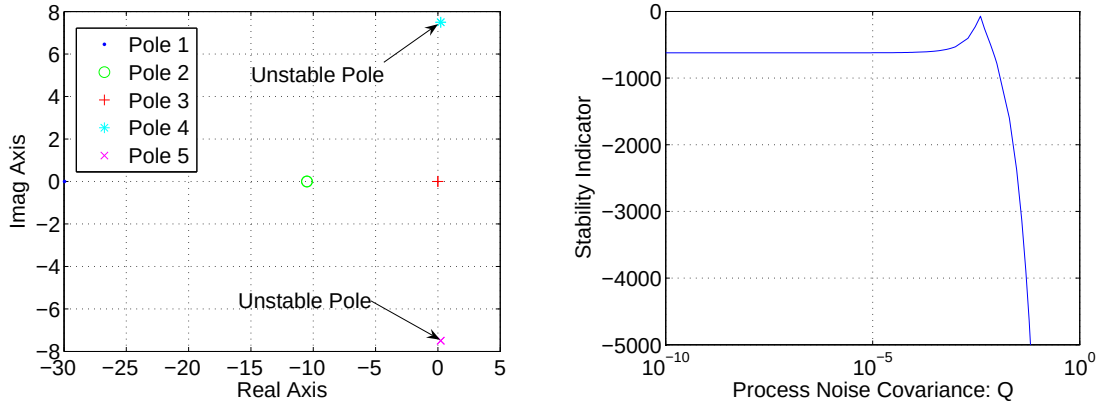

(a) System Closed-Loop Poles (b) Stability Indicator

Figure 23. Closed-Loop Stability Analysis: $Q = [1 \times 10^{-10} \ldots 1 \times 10^{2}]$ **and** $R = 1 \times 10^{3}$

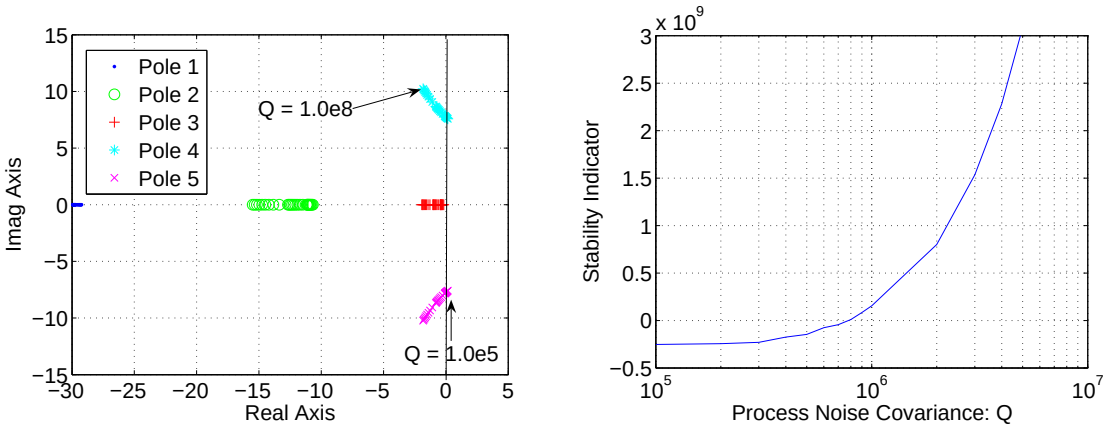

(a) System Closed-Loop Poles (b) Stability Indicator

Figure 24. Closed-Loop Stability Analysis: $Q = [1 \times 10^{5} \ldots 1 \times 10^{8}]$ **and** $R = 1 \times 10^{3}$

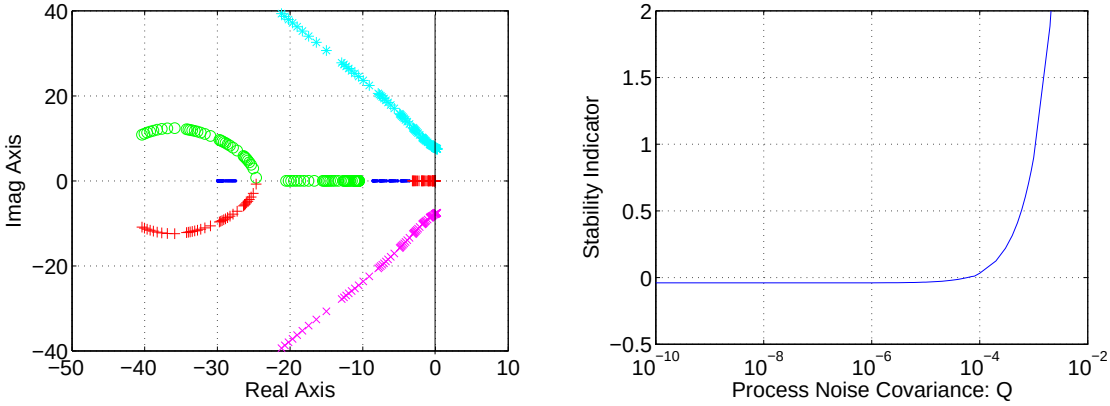

(a) System Closed-Loop Poles (b) Stability Indicator

Figure 25. Closed-Loop Stability Analysis: $Q = [1 \times 10^{-10} \ldots 1 \times 10^{2}]$ **and** $R = 1 \times 10^{-8}$

previous section. As revealed by the Lyapunov analysis, the closed-loop system stability is guaranteed only if the norm of process noise covariance value is greater then a certain lower bound. This lower bound on the process noise covariance norm is directly proportional to the model uncertainty and external disturbance while inversely proportional to the measurement noise covariance norm. Knowledge of this lower bound on process noise covariance can help to design an efficient disturbance accommodating controller using a Kalman filter.

VII. Conclusion

Disturbance can arise from system uncertainties and external undesirable inputs. The effective accommodation of these unmeasurable, persistently-acting disturbances is an important consideration in the design of virtually all control systems. A disturbance accommodating controller for nonlinear systems which utilizes an extended Kalman filter was presented in this paper. In this approach a control scheme is not explicitly derived, rather, existing control techniques are combined with a Kalman filter to determine the disturbance corrections which are used to update the nominal control input itself. Some advantages of this control approach include: the determined disturbance is a natural by-product of the state estimation, and it easily handles time-varying disturbances. One of the disadvantages of using the proposed disturbance accommodating control approach is that the stability of the controlled system using this technique is highly sensitive to the user selected process noise covariance value. The simulation results indicated that the closed-loop system is unstable for small values of process noise covariance. This due to the fact that when a small process noise covariance value is selected, the Kalman filter assumes there is no uncertainties associated with the assumed system model, thus minimizing the disturbance corrections to the nominal control input. Therefore the disturbance accommodating controller reduces down to just the nominal controller. Selecting a very large process noise covariance value will compel the EKF to completely rely upon the measurement signal. Therefore the noise associated with the measurement signal directly gets transmitted to the estimates. This could result in noisy control signal which could lead to problems such as chattering and controller saturation. The Lyapunov stability analysis conducted on a linear system, which utilizes the disturbance accommodating control approach with a linear Kalman filter, revealed that the asymptotic stability of the closed-loop system is guaranteed only if the norm of process noise covariance value is greater then a certain lower bound. This lower bound on the process noise covariance norm depends on the model uncertainties, external disturbances and the amount of noise associated with the measurements. Knowledge of this lower bound on process noise covariance can help to design efficient disturbance accommodating controllers.

References

[1]Johnson, C., "Accommodation of External Disturbances in Linear Regulator and Servomechanism Problems," *IEEE Transactions on Automatic Control*, Vol. AC-16, No. 6, December 1971, pp. 635–644.

[2]Johnson, C. and Kelly, W., "Theory of Disturbance-Utilizing Control: Some Recent Developments," *Proceedings of IEEE Southeast Conference*, Huntsville, AL, 1981, pp. 614–620.

[3]Johnson, C., "Adaptive Controller Design Using Disturbance Accommodation Techniques," *International Journal of Control*, Vol. 42, No. 1, 1985, pp. 193–210.

[4]Biglari, H. and Mobasher, A., "Design of Adaptive Disturbance Accommodating Controller with Matlab and Simulink," *NAECON, Proceedings of the IEEE National Aerospace and Electronics Conference (NAECON*, Dayton, OH, 2000, pp. 208–211.

[5]Mark J. Balas, R. F. and Mehiel, E., "Adaptive Control and Rejection of Persistent Disturbances: continuous and Discrete-Time," *Proceedings of AIAA GNC Conference and Exhibit*, Austin, TX, 2003.

[6]Joseph A. Profeta III, W. G. and Mickle, M. H., "Disturbance Estimation and Compesation in Linear Systems," *IEEE Transactions on Aerospace and Electronic Systems*, Vol. 26, No. 2, March 1990, pp. 225–231.

[7]Kim, J.-H. and Oh, J.-H., "Disturbance Estimation using Sliding Mode for Discrete Kalman Filter," *Proceedings of the* 37^{th} *IEEE Conference on Dicision and Control*, Tampa, FL, 1998, pp. 1918–1919.

[8]Crassidis, J. L., "Robust Control of Nonlinear Systems Using Model-Error Control Synthesis," *Journal of Guidance, Control, and Dynamics*, Vol. 22, No. 4, July-August 1999, pp. 595–601.

[9]Haberstock, J. and Johnson, C., "Disturbance-Utilizing Control for Linear Systems with Nonquadratic Performance Indices," *Proceedings of the Twentieth Southeastern Symposium on System Theory*, Charlotte, NC, 1988, pp. 280–287.

[10]Suarez, C. J., Kramer, B. R., Ayers, B., and Malcom, G., "Forebody Vortex Control fot Suppressing Wing Rock on a Highly-Swept Wing Configuration," *Proceedings of the* 10^{th} *Applied Aerodynamics Conference, (Palo Alto, CA)*, AIAA, Reston, VA, June 1992, AIAA Paper 92-2710.

[11]Morris, S. L., *A Video-Based Experimental Investigation of Wing Rock*, Ph.D. thesis, Texas A&M University, College Station, TX, 1989.

[12]Nayfeh, A. H., Elzebda, J. M., and Mook, D. T., "Analytical Study of the Subsonic Wing Rock Phenomenon for Slender Delta Wings," *Journal of Aircraft*, Vol. 26, No. 9, 1989, pp. 805–809.

[13]Luo, J. and Lan, C. E., "Control of Wing Rock Motion of Slender Delta Wings," *Journal of Guidance, Control, and Dynamics*, Vol. 16, No. 2, March-April 1993, pp. 225–231.

[14]Monahemi, M. M. and Krstic, M., "Control of Wing Rock Motion Using Adaptive Feedback Linearization," *Journal of Guidance, Control, and Dynamics*, Vol. 19, No. 4, July-August 1996, pp. 905–912.

[15]Araujo, A. D. and Singh, S. N., "Variable Structure Adaptive Control of Wing-Rock Motion of Slender Delta Wings," *Journal of Guidance, Control, and Dynamics*, Vol. 21, No. 2, March-April 1998, pp. 251–256.